Since January 2020 Elsevier has created a COVID-19 resource centre with free information in English and Mandarin on the novel coronavirus COVID-19. The COVID-19 resource centre is hosted on Elsevier Connect, the company's public news and information website.

Virus Research 202 (2015) 112–119

Contents lists available at ScienceDirect

Virus Research

journal homepage: www.elsevier.com/locate/virusres

Simian hemorrhagic fever virus: Recent advances

Margo A. Brinton*, Han Di, Heather A. Vatter

Georgia State University, Atlanta, GA, USA

ARTICLE INFO

Article history:
Available online 29 November 2014

Keywords:
Arterivirus
Simian hemorrhagic fever virus
PLP1
nsp1
Minor structural proteins
Infectious clone

ABSTRACT

The simian hemorrhagic fever virus (SHFV) genome differs from those of other members of the family Arteriviridae in encoding three papain-like one proteases (PLP1α, PLP1β and PLP1γ) at the 5′ end and two adjacent sets of four minor structural proteins at the 3′ end. The catalytic Cys and His residues and cleavage sites for each of the SHFV PLP1s were predicted and their functionality was tested in *in vitro* transcription/translation reactions done with wildtype or mutant polyprotein constructs. Mass spectrometry analyses of selected autoproteolytic products confirmed cleavage site locations. The catalytic Cys of PLP1α is unusual in being adjacent to an Ala instead of a Typ. PLP1γ cleaves at both downstream and upstream sites. Intermediate precursor and alternative cleavage products were detected in the *in vitro* transcription/translation reactions but only the three mature nsp1 proteins were detected in SHFV-infected MA104 cell lysates with SHFV nsp1 protein-specific antibodies. The duplicated sets of SHFV minor structural proteins were predicted to be functionally redundant. A stable, full-length, infectious SHFV-LVR cDNA clone was constructed and a set of mutant infectious clones was generated each with the start codon of one of the minor structural proteins mutated. All eight of the minor structural proteins were found to be required for production of infectious extracellular virus. SHFV causes a fatal hemorrhagic fever in macaques but asymptomatic, persistent infections in natural hosts such as baboons. SHFV infections were compared in macrophages and myeloid dendritic cells from baboons and macaques. Virus yields were higher from macaque cells than from baboon cells. Macrophage cultures from the two types of animals differed dramatically in the percentage of cells infected. In contrast, similar percentages of myeloid dendritic cells were infected but virus replication was efficient in the macaque cells but inefficient in the baboon cells. SHFV infection induced the production of pro-inflammatory cytokines, including IL-1β, IL-6, IL-12/23(p40), TNF-α and MIP-1α, in macaque cells but not baboon cells.

1. Introduction

SHFV is a member of the family Arteriviridae that also includes equine arteritis virus (EAV), lactate dehydrogenase-elevating virus (LDV), and porcine reproductive and respiratory syndrome virus (PRRSV) (Snijder and Kikkert, 2013). A related virus, wobbly possum disease virus (WPDV), was recently identified (Dunowska et al., 2012). Arterivirus genomes are positive-sense, single-stranded, polycistronic RNAs with a 5′ type I cap and a 3′ poly(A) tract (Snijder and Spaan, 2006). Among the arteriviruses, EAV has the shortest genome (12.7 kb) while SHFV has the longest (15.7 kb). The genome organization and replication strategies of arteriviruses are similar to those of coronaviruses. However, arterivirus genomes are about half the size of coronavirus genomes and the virions of the two virus groups differ in their structural protein compositions, capsid types (coronaviruses-helical and arteriviruses-spherical) and virion sizes.

Arteriviruses infect macrophages (MΦs) and dendritic cells (DCs) and have restricted host ranges; EAV infects horses and donkeys, PRRSV infects pigs, LDV infects mice and SHFV infects non-human primates (NHPs) (Snijder and Meulenberg, 1998). Disease symptoms associated with EAV and PRRSV infections include fever, respiratory disease, tissue necrosis and spontaneous abortions while LDV typically causes an asymptomatic, persistent infection (Snijder and Spaan, 2006). The majority of research on arteriviruses has focused on EAV and PRRSV due to the significant agricultural impact of the diseases they cause.

2. SHFV infections in NHPs

SHFV was first isolated in 1964 as the causative agent of hemorrhagic fever outbreaks associated with high mortality in macaque colonies in the United States and the USSR (Allen et al., 1968;

* Corresponding author. Tel.: +1 404 413 5388; fax: +1 404 413 5301.
E-mail address: mbrinton@gsu.edu (M.A. Brinton).

http://dx.doi.org/10.1016/j.virusres.2014.11.024
0168-1702/

Palmer et al., 1968; Tauraso et al., 1968; Shevtsova, 1969; Lapin and Shevtsova, 1971). African monkeys, such as baboons and African green, patas, guenons and colobus monkeys, are natural hosts of SHFV and typically develop asymptomatic, persistent infections with low level viremia (Bailey et al., 2014b; London, 1977; Lauck et al., 2011, 2013). SHFV-infected macaques develop fever, facial edema, anorexia, dehydration, depression and coagulation defects indicated by skin petechiae, retrobulbar hemorrhages and subcutaneous hematomas. Death occurs 7–13 days after infection (Allen et al., 1968; Palmer et al., 1968; London, 1977). The clinical signs and disease course closely resemble those induced in macaques by other hemorrhagic fever virus infections, such as Ebola Zaire, Marburg, and Lassa (Mahanty and Bray, 2004; Bray and Geisbert, 2005). The presence of persistently infected African NHPs in the NIH primate colony that had several SHFV outbreaks and the use of the same needle for tattooing or tuberculosis testing of multiple NHPs of African and Asian origin are thought to have resulted in inadvertent virus transmission from an African animal to macaques (Allen et al., 1968; Palmer et al., 1968; Tauraso et al., 1968). SHFV is typically transmitted between African NHPs during fighting but can spread efficiently among macaques by both direct and indirect contact (London, 1977; Renquist, 1990).

Based on an unpublished number of test animals, it was previously estimated that 1% of baboons, 1% of African green monkeys and 10% of patas monkeys are SHFV-positive (London, 1977). In a recent study, sera/plasma samples from 205 baboons from a US colony were tested for SHFV using RT-PCR assays targeted to two conserved sequence regions (Vatter et al., 2015). Of the wild-caught Olive baboons tested, 14.2% were positive for SHFV. However, because sera samples collected at the time of capture were not available, it is not known whether these animals were infected in the wild or after capture. Nineteen percent of the opportunistically sampled animals living in the colony were SHFV-positive. However, because most of the colony animals tested were males that were being treated for lacerations obtained during fighting, the percentage of SHFV-positive animals in the entire colony is expected to be lower. None of the SHFV positive baboons showed any signs of disease. Infections lasting >10 years were documented using serial archived sera samples and the viremia levels were consistently low (100–1000 PFU/ml).

3. SHFV isolates

The outcomes of experimental infections of patas monkeys with one of four previous SHFV isolates indicated differences in their biological properties (Gravell et al., 1986). LVR was isolated from a stump tail macaque that died of hemorrhagic fever disease (Tauraso et al., 1968), P-248 was isolated from a feral, persistently infected patas monkey, P-180 was isolated from a patas monkey that died from an SHFV infection, and P741 was isolated from a rhesus macaque that died after inoculation of SHFV from an asymptomatic persistently infected patas monkey. Infection of patas monkeys with two of the isolates (LVR and P-180) produced acute infections characterized by transient clinical signs of hemorrhagic disease with p-180 causing more severe disease that was only rarely fatal. Infection of patas monkeys with either P-248 or P741 produced asymptomatic, long-term persistent infections. Acutely infected animals produced high levels of anti-viral antibody while antibody titers in persistently infected animals were low. Lytic infections were induced by LVR in MA-104 cells, a rhesus macaque kidney cell line, as well as in both patas and rhesus peritoneal MΦs. P-180 could lytically infect both types of MΦs but not MA-104 cells while P-248 and P-741 could lytically infect only rhesus macaque MΦs. All four of these isolates efficiently induced acute fatal hemorrhagic fever disease in macaques. EAV and PRRSV can also efficiently infect MA104 cells. The MΦ-restricted protein sialoadhesion (CD169) mediates attachment and internalization by clathrin-mediated endocytosis of EAV and PRRSV (Van Breedam et al., 2010). CD163 was identified as an arterivirus co-receptor required for nucleocapsid release from endosomes and is also monocyte-macrophage lineage restricted (Welch and Calvert, 2010). MA104 cells express CD163 and CD151 but not sialoadhesin. It was recently reported that SHFV LVR enters MA104 cells by clathrin-mediated endocytosis and that treatment of MA104 cells with anti-CD163 antibody decreased SHFV replication (Cai et al., 2014).

Only the prototype SHFV isolate, LVR v42-0/M6941, survived from the earlier studies of SHFV (Tauraso et al., 1968). The species of African NHP from which LVR originated is not known for certain but patas monkeys housed in the same facility were subsequently shown to be persistently infected with SHFV and the source of the SHFV initiating later epizootics in macaques in the same facility (London, 1977). A complete sequence of the SHFV LVR genome was obtained in the early 1990s by sequencing “shot gun” clones using older methods (GenBank Accession number AF180391.1). During the construction of the first SHFV infectious clone, nucleotide differences were detected between the RT-PCR amplified cDNA fragments used to construct the full length clone and the GenBank sequence. The SHFV LVR genome RNA was also subjected to 454 sequencing and the same 18 nt differences compared to the GenBank sequence were detected by 454 genomic sequencing and individual fragment sequencing. The GenBank sequence was updated (GenBank Accession number AF180391.2).

Although inoculation of a low dose of SHFV LVR in sera or culture fluid by the intramuscular route consistently induced severe hemorrhagic disease in macaques in the 1960s (Palmer et al., 1968; Tauraso et al., 1968), no correlation between SHFV LVR dose (50–500,000 PFU) and hemorrhagic disease induction in macaques was observed in a 2011 study and the majority of the animals (12 of 16) that did not survive were found to have bacterial sepsis (Johnson et al., 2011b). The inoculum used in this study was generated by three freeze–thaw cycles of infected MA104 cells. Activation of cell RNA sensors by the large amounts of cell and viral [genomic and subgenomic (sg)] RNAs in these lysates may have induced a strong host antiviral response that contributed to the decreased efficiency of hemorrhagic disease induction observed. Also, defective SHFV genomes present in the LVR stock used may have reduced the efficiency of virus replication (Vatter et al., 2015).

SHFV isolates obtained from two SHFV-positive Olive baboons (B11661 and B11662) that were housed together only in the early 1990s and persistently infected >10 years were amplified by a single passage in primary rhesus macaque MΦs and then the genomes were 454 sequenced (Vatter et al., 2015). The two sequences obtained were very similar to each other, differing at 15 nt positions within the 15.7 kb genome. Surprisingly, these genome sequences were also very similar (differing at 7 or 10 unique positions, respectively) to that of a three times serially plaque-purified stock of SHFV LVR grown in MA104 cells. Four Japanese macaques injected intravenously with 100 PFU of B11661 developed severe hemorrhagic fever disease, characterized by high level viremia, the production of pro-inflammatory cytokines, elevation of tissue factor and coagulopathy, but showed no evidence of bacterial sepsis. Infected MΦs were detected in liver and spleen tissue sections using antibody to viral nonstructural proteins and the MΦ marker CD68. SHFV infection in macaques has been proposed as a BSL2 model for viral hemorrhagic fever disease (Johnson et al., 2011b).

Another recent study sequenced SHFV genomes obtained from wild Mikumi yellow baboons and captive Olive baboons in the same US primate facility used for the study described above and found them to be divergent (Bailey et al., 2014a,b). SHFV genome sequences obtained from additional wild species of African NHPs, red colobus and red-tailed guenons, have also been reported (Lauck et al., 2013; Bailey et al., 2014a,b). Two different strains

of SHFV (krc1 and krc2) were isolated from red colobus animals and sequence diversity was detected among isolates of the same strain from different infected animals. One animal was found to be co-infected with both SHFV strains. No signs of disease were observed in SHFV-infected red colobus, even though the viremia levels were high (10^6–10^7 RNA copies/ml of plasma). It is not yet known whether these SHFV isolates can infect macaques and induce hemorrhagic fever disease.

3.1. Characteristics of SHFV LVR infections in primary cells from disease resistant baboons and disease susceptible macaques

It was previously reported that pro-inflammatory cytokines released from Ebola infected macaque MΦs and DCs upregulate tissue factor and induce disseminated intravascular coagulopathy (Bray and Geisbert, 2005). The ability of an SHFV LVR infection to induce proinflammatory cytokine production was compared in MΦs and myeloid (m) DCs differentiated in culture from peripheral blood mononuclear cells (PBMCs) collected from disease resistant baboons and disease susceptible macaques (Vatter and Brinton, 2014). Both viral RNA replication and virion production were more robust in macaque MΦs and mDCs than in baboon cells (Table 1). Approximately ~90% of macaque MΦs but only 10% of baboon MΦs were productively infected but the intracellular dsRNA fluorescence signal was similarly bright in the cells from both types of NHPs. In contrast, a similar percentage (~50%) of baboon and macaque mDCs were infected but the intensity of the intracellular dsRNA signal was much higher in macaque mDCs than baboon mDCs suggesting that the higher yield of SHFV produced by macaque mDCs was due to more efficient intracellular virus replication. The mechanisms involved in the observed variations in cell susceptibility have not yet been analyzed.

Consistent with the observed induction of hemorrhagic fever disease by SHFV infection in macaques, SHFV infection of cultured macaque but not of baboon MΦs and mDCs induced the production of pro-inflammatory cytokines, such as IL-1β, IL-6, IL-12/23(p40), TNF-α and MIP-1α (Vatter and Brinton, 2014). UV-inactivated SHFV induced only transient production of IL-6 and IL-1β indicating that early stages of the virus lifecycle can induce this response but that sustained pro-inflammatory cytokine production requires virus replication (Vatter and Brinton, 2014). IL-10 signaling leads to upregulation of suppressor of cytokine signaling 3 (SOCS3) (Moore et al., 2001). Cultured baboon MΦs and mDCs expressed higher basal levels of IL-10 than macaque cells and the levels of both the inducible IL-10 receptor subunit 1 (IL-10R1) and SOCS3 were upregulated in SHFV-infected baboon MΦs and mDCs. In contrast, in SHFV-infected macaque MΦs and mDCs, the levels of IL-10R1 were downregulated with time after infection and SOCS3 expression was not induced. Treatment of macaque MΦs and mDCs with recombinant human IL-10 starting prior to or at the time of infection with SHFV suppressed IL-6 and MIP-1α but not TNF-α production without altering viral yields or cell viability. Treatment of baboon cells with anti-IL-10 antibody did not result in the production of proinflammatory cytokines and SOCS3 expression was upregulated prior to the upregulation of IL-10R1 suggesting that SOCS3 expression may be induced by SHFV infection.

4. Arterivirus Genome Structure

The arterivirus major and minor structural proteins are encoded within the 3′ one-third of the genome and are translated from a nested set of 5′ and 3′ coterminal subgenomic mRNAs (sg mRNAs) (Zeng et al., 1995; Godeny et al., 1998; Snijder and Spaan, 2006). The 5′ two-thirds of the genome encodes two polyproteins 1a and 1ab. Polyprotein 1ab is produced when a −1 ribosomal frameshift occurs on a slippery sequence located near the polyprotein 1a stop codon (Snijder and Spaan, 2006). A second frameshift (−2) can occur in nsp2 producing a truncated nsp2 protein with a different C-terminal sequence (nsp2TF) (Fang et al., 2012). Polyproteins 1a and 1ab are posttranslationally cleaved by viral proteases to generate the nonstructural proteins (nsps) involved in replication and transcription of the viral genome and sg mRNAs (Snijder and Meulenberg, 1998; Beerens et al., 2007). The SHFV genome encodes additional proteins at both its 5′ and 3′ ends compared to the genomes of the other known arteriviruses.

The nsp1 proteins are encoded at the N-terminus of polyproteins 1a and are cleaved from the polyprotein by viral papain-like protease 1 (PLP1) domains. All of the arterivirus nsp1 proteins function as interferon pathway antagonists, inhibiting IRF-3 and NF-κB mediated IFNβ promoter activity as well as the ISRE promoter activity (Beura et al., 2010; Fang and Snijder, 2010; Kim et al., 2010; Song et al., 2010; Beura et al., 2012; Han et al., 2014). The N-terminal zinc-finger domain in EAV nsp1 and PRRSV nsp1α was shown to regulate sg mRNA and genome transcription abundance (van Dinten et al., 1997; Kroese et al., 2008; Nedialkova et al., 2010; Snijder and Kikkert, 2013).

5. Arterivirus proteases

The arterivirus ORF1a polyprotein encodes multiple proteases: PLP1 domains in the nsp1 region, a PLP2 domain in nsp2, and the main serine protease domain in nsp4 (Snijder and Spaan, 2006). Arterivirus PLP2s are similar to coronavirus PLPs (PLP1, PLP2, and PLpro) in having a catalytic Cys-His-Asp triad and the ability to cleave both *in cis* and *in trans* (Mielech et al., 2014). In contrast, arterivirus PLP1s have a Cys-His catalytic tandem (Sun et al., 2009;

Table 1
Comparison of SHFV LVR infection and replication efficiencies in disease-resistant baboon and disease-susceptible macaque cells.

	Macaque MΦ	Baboon MΦ
Virus peak titer	8×10^4 PFU/ml by 36 h[a]	7×10^2 PFU/ml by 12 h[a]
Intracellular viral genome RNA levels	High[a]	Low[a]
Cell viability after infection	Decreased by~25% at 12 h and by 80% at 48 h[a]	Decreased by ~13% at 24 h and no further decrease by 48 h[a]
Infection rate	~90% by 24 h[b]	~10% by 24 h[b]
Virus replication efficiency (dsRNA)	High[b]	High[b]
	Macaque mDCs	**Baboon mDCs**
Virus peak titer	9×10^4 PFU/ml by 24 h[a]	2×10^2 PFU/ml by 8 h[a]
Intracellular viral genome RNA levels	High[a]	Low[a]
Cell viability after infection	Decreased by ~50% at 24 h and by ~80% at 48 h[a]	Decreased by ~25% at 12 h but no further decrease by 48 h[a]
Infection rate	~45% by 8 h[b]	~50% by 8 h[b]
Virus replication efficiency (dsRNA)	High[b]	Low[b]

[a] Infections were done with a MOI of 1.
[b] Infections were done with a MOI of 10.

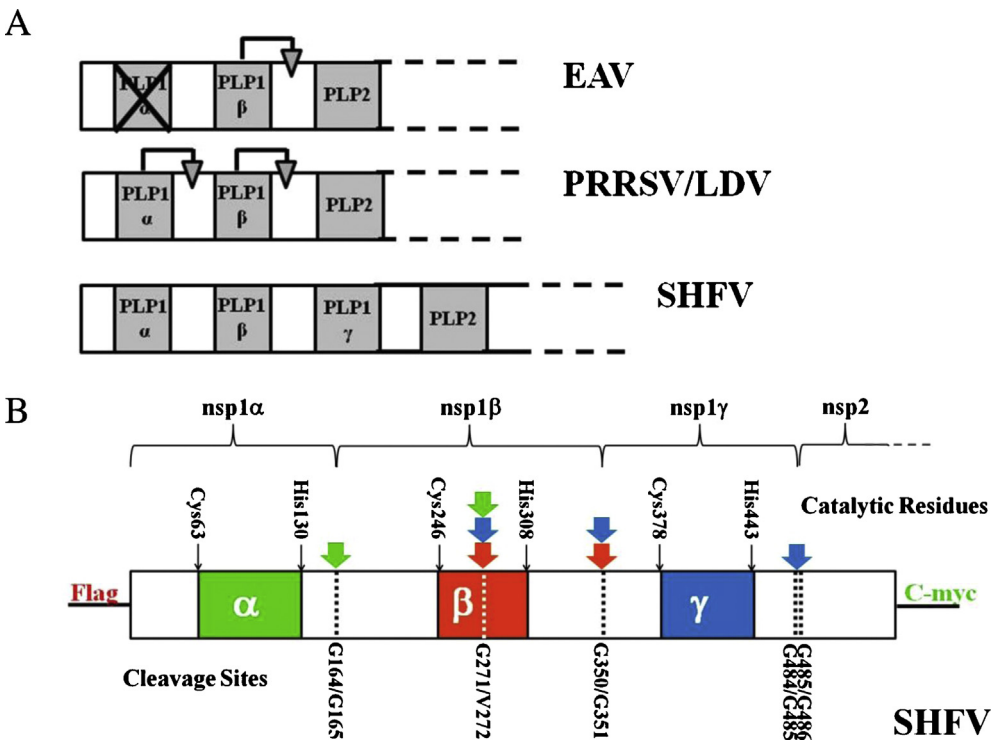

Fig. 1. Diagram of the PLP1 domains and cleavage sites in the SHFV nsp1 region. (A) The papain-like protease 1 and 2 domains in the N-terminal region of the 1a polyprotein are indicated by gray boxes. The EAV PLP1α is inactive due to substitution of the catalytic Cys. Demonstrated cleavage *in cis* at a single downstream site is indicated by arrows. (B) A pTnT vector containing the N-terminal 1725 nts of the SHFV ORF1a was constructed with an N-terminal Flag tag and a C-terminal c-Myc tag and used to analyze autocleavage *in vitro*. The locations of the predicted PLP1 domains are indicated by colored boxes and the locations of the catalytic residues are indicated by thin arrows. The cleavage sites used are indicated by dotted lines and the PLP1s that cleave at each site in *in vitro* autoprocessing reactions are indicated by color coordinated thick arrows. The cleavage products, nsp1α, nsp1β, nsp1γ, and the N-terminal part of nsp2, are indicated by brackets.

Xue et al., 2010). EAV, LDV and PRRSV PLP1s were shown to cleave exclusively *in cis* at a single site downstream of the catalytic domain (Snijder and Spaan, 2006). All of the coronavirus PLPs and the arterivirus PLP2s also have deubiquitinating and deISGylating activities (van Kasteren et al., 2013; Mielech et al., 2014). Most coronavirus PLPs cleave at a canonical -Leu-X-Gly↓Gly site but the cleavage sites of arterivirus PLPs are not well conserved (Sun et al., 2009; Xue et al., 2010; Mielech et al., 2014). Autocleavage by LDV and PRRSV PLP1α and PLP1β generate nsp1α and nsp1β, respectively (den Boon et al., 1995; Sun et al., 2009; Xue et al., 2010) (Fig. 1A). The EAV PLP1α domain is inactive due to a Lys substitution of the catalytic Cys residue and a single nsp1 fusion protein is produced (Snijder et al., 1992; Ziebuhr et al., 2000).

6. Functional analysis of the SHFV PLP1s

SHFV is unique among arteriviruses in encoding a longer nsp1 region containing three predicted PLP1 domains (PLP1α, PLP1β, and PLP1γ) (Fig. 1A). The SHFV LVR nsp1 sequences were homology modeled on crystal structures of PRRSV nsp1α and nsp1β (Sun et al., 2009; Xue et al., 2010; Vatter et al., 2014b). SHFV nsp1α modeled well on the PRRSV nsp1α structure and SHFV nsp1β modeled well on the PRRSV nsp1β structure. SHFV nsp1γ was modeled on both the PRRSV nsp1α and nsp1β structures and appeared to be more similar to PRRSV nsp1α than to nsp1β. The catalytic residues of other arterivirus PLP1s were previously identified as a Cys and a His located about 60 amino acids downstream. In all previously studied active arterivirus PLP1s, a Trp follows the catalytic Cys (den Boon et al., 1995; Sun et al., 2009; Xue et al., 2010). Alignment of the three SHFV PLP1 sequences with each other using a conserved GV[Q/T]G motif as an anchor (Vatter et al., 2014b) predicted Cys246 as a catalytic residue of PLP1β and Cys378 as a catalytic residue of PLP1γ. Each of these Cys residues was adjacent to a Trp and located 62 and 64 aa upstream, respectively, of the predicted catalytic His. In PLP1α, the only Cys adjacent to a Trp was Cys115 located only 14 amino acids upstream of the predicted catalytic His. Cys63 located 67 amino acids upstream of the predicted catalytic His aligned with the predicted catalytic Cys residues of SHFV PLP1β and PLP1γ but was adjacent to an Ala. Alignment of SHFV, PRRSV and LDV PLP1α sequences also predicted Cys63 as the catalytic Cys. The alignments predicted that SHFV PLP1α cleaved at either Gly170/Thr171 or Gly164/Gly165, that PLP1β cleaved at Gly350/Gly351 and that PLP1γ cleaved at Gly484/Gly485.

In vitro autocleavage products of wild type and mutant polyproteins consisting of the SHFV LVR nsp1 region plus the N-terminal part of nsp2 with an N-terminal Flag tag and a C-terminal c-Myc tag were analyzed (Vatter et al., 2014b). In addition to the expected cleavage products, a ~30 kDa band was consistently detected in the wild type lysate as well as the Flag and c-Myc immunoprecipitation lanes, suggesting the existence of an extra cleavage site within the PLP1β catalytic domain that generated N- and C-terminal ~30 kDa cleavage products. Substitution of Cys63 with Ala in PLP1α abrogated cleavage between nsp1α and nsp1β and substitution of Cys378 in PLP1γ abrogated cleavage between nsp1γ and nsp2, identifying these Cys as functional catalytic residues (Fig. 1B) (Vatter et al., 2014b). However, substitution of Cys246 with Ala in PLP1β reduced but did not inhibit cleavage between nsp1β and nsp1γ suggesting that Cys246 is a PLP1β catalytic residue but that another PLP1 can also cleave at the nsp1β/nsp1γ junction. Inefficient cleavage at the nsp1α/nsp1β junction as well as within nsp1β by PLP1α was observed when both the PLP1β and PLP1γ catalytic Cys residues were substituted with Ala. Efficient cleavage at the nsp1β/nsp1γ junction as well as within nsp1β by PLP1β was observed when the catalytic Cys residues of both PLP1α and PLP1γ were mutated. However, efficient cleavage at the nsp1γ/nsp2 junction, within nsp1β and also at the nsp1β/nsp1γ junction by PLP1γ

was observed when the PLP1α and PLP1β catalytic Cys residues were mutated indicating that SHFV PLP1γ can cleave at upstream sites as well as at a downstream site (Fig. 1B).

Constructs with the −1 and −2 amino acids of each predicted cleavage site substituted were used to functionally identify the SHFV PLP1 cleavage sites (Vatter et al., 2014b). Two putative cleavage sites were predicted for PLP1α; no cleavage at the nsp1α/nsp1β junction was detected when Gly164/Gly165 were substituted while substitution of the Gly171/Thr172 site only partially reduced cleavage, suggesting that the Gly164/Gly165 site is the preferred cleavage site at the nsp1α/nsp1β junction (Fig. 1B). This finding was supported by a mass spectroscopy analysis of the immunoprecipitated nsp1α cleavage product that detected ten trypsin generated peptides ending at aa164 and only one peptide ending at aa171. Substitution of the predicted Gly350/Gly351 site resulted in loss of cleavage at the nsp1β/nsp1γ junction, indicating this is the cleavage site used. Three adjacent Gly residues are present at the predicted cleavage site between nsp1γ and nsp2. Substitution of either Gly484/Gly485 or Gly485/Gly486 resulted in loss of cleavage between nsp1γ and nsp2. Mass spectroscopy analyses of immunoprecipitated cleavage products nsp1α + β and nsp1α + β + γ confirmed the locations of the cleavage sites at the nsp1β/nsp1γ and nsp1γ/nsp2 junctions. Substitution of the Gly271/Val272 site within nsp1β resulted in the loss of cleavage within nsp1β, indicating that this site can be cleaved in *in vitro* reactions.

Analysis of SHFV nsp1 region autoprocessing in infected cells by Western blotting using SHFV nsp1α-, nsp1β- (N- or C-terminal) or nsp1γ-specific antibodies detected only the mature nsp1α, nsp1β and nsp1γ proteins, respectively (Vatter et al., 2014b). The lack of detection of any intermediate precursor bands or truncated nsp1β proteins suggested that rapid processing of the nsp1 polyprotein occurs in infected cells. Cleavage at the Gly271/Val272 site within nsp1β in the *in vitro* assays but not in infected cells could be due to misfolding of some of the *in vitro* translated polyproteins and/or the lack of posttranslational modifications and/or chaperones.

A recent study on arterivirus nsp1 proteins used SHFV nsp1 expression constructs made from a different stock of SHFV LVR than the one used in the study described above to analyze autocleavage in HeLa cells (Han et al., 2014). This study predicted Cys 115 as a catalytic residue of PLP1α and did not observe cleavage at the nsp1α/nsp1β junction.

7. Arterivirus structural proteins

Arteriviruses differ from coronaviruses in having a spherical nucleocapsid composed of interacting nucleocapsid (N) protein dimers. The capsid is surrounded by an envelope that contains two major envelope proteins, the non-glycosylated membrane (M) protein and the major glycoprotein (GP5), which form disulfide-linked heterodimers (Delputte et al., 2002, 2007). Three minor glycoproteins (GPs), GP2, GP3 and GP4, form a complex that is located periodically on the virion envelope (Snijder and Spaan, 2006; Tian et al., 2012). Another minor structural protein E forms oligomers in the virion envelope and is thought to function as an ion-channel during viral entry (Snijder et al., 1999; Lee and Yoo, 2006). An additional recently discovered minor structural protein 5a was detected in purified PRRSV particles and inhibition of 5a expression reduced EAV yields (Johnson et al., 2011a; Sun et al., 2013). SHFV is unique among the arteriviruses in encoding two adjacent sets of four minor structural proteins (Godeny et al., 1998). These genes, listed in their order from 5′ to 3′ in the genome, were recently renamed GP2′, E′, GP3′, GP4′ and E, GP2, GP3, GP4 (Fig. 2A). Notably, the order of the open reading frames (ORFs) encoding the GP2 and E protein orthologs differ between the two sets (Fig. 2B) (Snijder and Spaan, 2006).

8. Analysis of SHFV sg mRNAs

EAV encodes a single set of the four minor structural proteins that are produced from three sg mRNAs because GP2 and E are both expressed from the bicistronic sg mRNA 2 (van Berlo et al., 1982; Snijder and Meulenberg, 1998; Snijder et al., 1999). SHFV encodes two adjacent sets of the four minor structural proteins and six sg mRNAs were expected for their expression (Fig. 2C). However, the leader-body junction sequence for an SHFV GP3′ sg mRNA was not detected in a previous study suggesting that SHFV GP2′ and GP3′

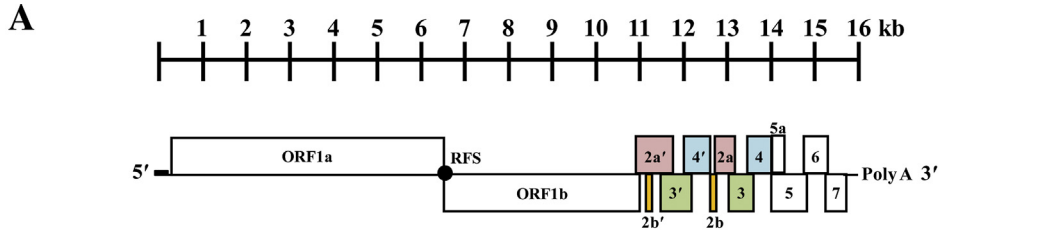

B

Duplicated sets of minor structural proteins	
ORF2a′ (10953nt-11798nt) GP2′ (281aa)	ORF2b (12555nt-12797nt) E (80aa)
ORF2b′ (11047nt-11331nt) E′ (94aa)	ORF2a (12595nt-13239nt) GP2 (214aa)
ORF3′ (11486nt-12100nt) GP3′ (204aa)	ORF3 (13089nt-13628nt) GP3 (179aa)
ORF4′ (11938nt-12555nt) GP4′ (205aa)	ORF4 (13451nt-13999nt) GP4 (182aa)

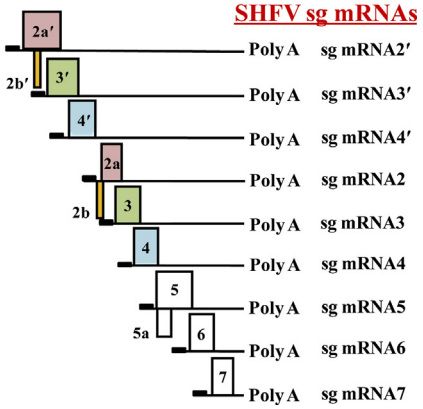

Fig. 2. SHFV genome and sg mRNA ORFs. (A) Schematic representation of the genes encoded by the SHFV genome. (B) List of the two sets of minor structural protein ORFs and proteins. (C) Schematic representation of the SHFV sg mRNAs and the ORFs that they encode. Each of the SHFV sg mRNAs contains a 5′ leader sequence indicated by a black box.

were expressed from a bicistronic sg mRNA 2′ (Godeny et al., 1998). The subsequent discovery of an ORF for the E′ protein which overlaps the GP2′ ORF and the demonstration of bicistronic expression of E and GP2 from the EAV sg mRNA 2 (Snijder et al., 1999) made it unlikely that three minor structural proteins, GP2′, E′ and GP3′, would be expressed from the SHFV sg mRNA2′. A recent Northern blotting analysis of the sg mRNAs produced in infected MA104 cells detected six minor structural protein sg mRNAs including one of the size predicted for a separate GP3′ sg mRNA (sg mRNA 3′) (Vatter et al., 2014a). The existence of sg mRNA 3′ was confirmed by leader-body sequencing data. The ORFs for GP2′, E′ and GP3′ were renamed ORF2a′, ORF2b′ and ORF3′, respectively (Fig. 2B). The identification of sg mRNA3′ for GP3′ led to the interesting observation that the relative abundance of the corresponding sg mRNAs in the duplicated sets of the SHFV minor structural proteins was similar, with sg mRNAs 2′ and 2 being more abundant and sg mRNAs 3′, 3, 4′ and 4 being less abundant. This finding indicated that regulation of the expression of the individual minor structural protein sg mRNAs in the duplicated sets is conserved. However, the different order of the ORFs for the GP2 and E orthologs in the two sets suggests that the second set of SHFV minor structural proteins was not generated by a simple gene duplication event.

9. Regulation of SHFV RNA replication

Little work has so far been done on the viral and cell proteins and *cis* acting viral RNA elements involved in regulating SHFV RNA replication. However, RNA structures in the 3′ noncoding region (NCR) of the genome and the 3′ terminal region of the minus strand (−) RNA were previously predicted and cell proteins binding to these RNA regions that may be involved in regulating initiation of RNA synthesis were reported (You-Kyung and Brinton, 1998; Maines et al., 2005). Two cell proteins, p56 and p42, that bound specifically to an SHFV 3′(+)NCR RNA probe were identified as polypyrimidine tract-binding protein (PTB) and fructose bisphosphate aldolase A, respectively. PTB binding sites in the SHFV 3′(+)SL structure were mapped to a terminal loop and a bulged region and the aldolase A binding site to a region near the top of the 3′SL. Four SHFV 3′(−) RNA binding cell proteins (103, 86, 55, and 36 kDa) were detected in UV-induced cross-linking assays, and three of these proteins (103, 55, and 36 kDa) were also detected by Northwestern blotting assays. The binding sites for these four cellular proteins were mapped to the region between nt 117 and 184 from the 3′ end of the minus strand RNA. This 68-nt sequence was predicted to form two stem-loops, SL4 and SL5. Additional data obtained with the (+) and (−) 3′ terminal RNAs of other arteriviruses suggested that the RNA elements interacting with the identified cell proteins are conserved among arteriviruses.

10. Functional analysis of the two sets of SHFV minor structural proteins

Mutant SHFV infectious clones lacking the expression of either one of the minor structural proteins or of a pair of minor structural protein orthologs were made (Vatter et al., 2014a). None of these clones produced infectious virus. However, the ability of each clone to produce extracellular virions was assessed by quantitative real-time RT-PCR of extracellular viral RNA levels. Cells transfected with the ΔGP4′, ΔGP2 or ΔGP3 mutant infectious clone RNAs produced a sustained low level of extracellular viral RNA beginning at 24 h after transfection (Table 2). In contrast, after transfection of wildtype infectious clone RNA, extracellular viral RNA increased dramatically starting at 96 h after transfection. The lack of amplification of extracellular viral RNA at later times observed for all of the mutants indicated that the extracellular virus particles produced were non-infectious. The ΔGP4 infectious clone RNA also produced a low level of extracellular viral RNA beginning at 24 h after transfection, but the level was not sustained indicating a potential role for GP4 in virion stability. The ΔGP2′, ΔGP3′, ΔE′ and ΔE mutant infectious clone RNAs did not produce extracellular viral RNA above background levels suggesting that each of these proteins plays an essential role in virus replication or virion production. No extracellular viral RNA production was detected from MA104 cells transfected with any of the double mutant RNAs. No intracellular viral proteins were detected in lysates from any of the mutant RNA transfected cells by Western blotting, which is consistent with a lack of virus spread. Although the abundance of sg mRNA orthologs for the duplicated sets of SHFV minor structural proteins is similar, the functions of the ortholog proteins are not redundant. The finding that both sets of minor structural proteins are required for efficient production of infectious extracellular virus indicates that SHFV virus production and virion structure are more complex than those of other known arteriviruses.

Table 2
Summary of the SHFV minor structural protein functions.

Functions	SHFV minor structural proteins
Virion production	GP2′, GP3′, E, and E′
Virion infectivity	GP2, GP3, GP4, and GP4′
Virion stability	GP4

11. Conclusions

SHFV typically causes benign persistent infections in African NHPs that are natural hosts but fatal hemorrhagic fever disease in Asian macaques that are not natural hosts. MΦs cultures from the two types of animals differed in the percentage of susceptible cells present while mDCs from the two animals differed in their ability to efficiently replicate virus. Consistent with the different symptoms observed in SHFV infected African NHPs and macaques, SHFV infection of cultured macaque MΦs and mDCs induced pro-inflammatory cytokine production while infections in baboon cells did not. The data suggest that there is a balance between upregulation of cell anti-viral and inflammatory responses and viral-mediated counteraction/modulation of these responses that is beneficial to both the host and the virus in African NHPs but not in macaques. All previous isolates of SHFV caused severe hemorrhagic fever disease in macaques but varied in their ability to cause signs of hemorrhagic disease that was rarely fatal in patas monkeys. A new SHFV isolate from persistently infected baboons was able to lytically infect rhesus macaque MΦs and MA104 cells and caused long term asymptomatic persistent infections in baboons but fatal hemorrhagic fever disease in macaques. Although divergent SHFV genome sequences obtained from additional NHP species have recently been reported, data from experimental infection studies with these isolates in different types of NHPs and cells have not yet been reported.

The SHFV genome encodes five additional proteins compared to other known arteriviruses. The additional nsp1 protein nsp1γ was predicted to be structurally more similar to PRRSV nsp1α than to PRRSV nsp1β. Also, PLP1γ is able to cleave at upstream as well as downstream sites, which is a characteristic of the PLP2s but not PLP1s of other arteriviruses. Arterivirus PLP2s have a Cya-His-Asp catalytic triad and deubiquitinating as well as deISGylating activities in addition to protease activity. SHFV PLP1γ has a Cys-His catalytic dyad and is not predicted to have deubiquitinating or deISGylating activity. SHFV nsp1γ may have originated by a duplication of nsp1α. It is possible that SHFV PLP1α may also be able to cleave upstream but due to its location at the 5′ end of the 1a polyprotein, this ability was not tested. Sequence alignment indicated that the

three SHFV PLP1s are more similar to each other than to those of other arteriviruses. Additional functional studies of the SHFV PLP1s, including analysis of possible *trans* cleavage activities, as well as crystal structures of the three SHFV nsp1s are needed to provide insights about the origin of the additional SHFV nsp1 region.

A duplicated set of four additional minor structural proteins is encoded in the 3′ end of the SHFV genome. The finding that each of the minor structural proteins from both sets is required for the production of infectious SHFV suggests that the SHF virion composition is more complex than that of other known arteriviruses. Cells transfected with mutant viral RNAs that did not express GP2′, GP3′, E, or E′ did not produce extracellular virus particles suggesting that these proteins have essential functions during earlier stages of the virus life cycle. However, some or all of these proteins may also be functionally important for virion infectivity. The EAV, PRRSV and LDV E proteins have a conserved N-terminal myristoylation site (Thaa et al., 2009). The observation of a decrease in virus infectivity and plaque size but not in the yield of extracellular virions when myristoylation was inhibited in EAV-infected cells suggested that E protein myristoylation is required for virion infectivity but not for virion budding (Thaa et al., 2009). This finding is consistent with E protein ion channel function being required for virion entry. The SHFV E protein sequence contains the conserved N-terminal myristoylation site but the SHFV E′ protein sequence does not. Both of the SHFV E proteins appear to have intracellular functions during the virus replication cycle but one or both may also function during virion entry. The SHFV E protein is more homologous to the EAV and LDV E proteins and the orientation of the overlapping E and GP2 ORFs in these three genomes is similar. However, the SHFV E′ is more homologous to the PRRSV E and the SHFV E′ and GP2′ ORFs as well as the PRRSV E and GP2 ORFs are in the opposite orientation (Fig. 2). All of these data support acquisition of an additional set of minor SHFV structural proteins by a recombination event with the genome of another arterivirus than by a "duplication" recombination event between SHFV genomes. All of the newly discovered SHFV genomes in additional species of NHPs that have been recently sequenced encode two similar sets of minor structural proteins indicating that the addition of the second set of genes is not a recent event. The identity of the ancestral arterivirus that contributed the additional set of SHFV minor structural proteins and the circumstances under which a co-infection occurred are not known.

Acknowledgements

This work was supported by a Public Health Service Research Grant AI073824 to M.A.B from the National Institute of Allergy and Infectious Diseases, National Institutes of Health. H.A.V. and H.D. were supported by Molecular Basis of Disease Fellowships from Georgia State University. This project used biological materials from the Southwest National Primate Research Center (P51OD011133) and from the Yerkes National Primate Research Center Comparative AIDS Core (P51OD011132).

References

Allen, A.M., Palmer, A.E., Tauraso, N.M., Shelokov, A., 1968. Simian hemorrhagic fever. II. Studies in pathology. Am. J. Trop. Med. Hyg. 17 (3), 413–421.

Bailey, A.L., Lauck, M., Sibley, S.D., Pecotte, J., Rice, K., Weny, G., Tumukunde, A., Hyeroba, D., Greene, J., Correll, M., Gleicher, M., Friedrich, T.C., Jahrling, P.B., Kuhn, J.H., Goldberg, T.L., Rogers, J., O'Connor, D.H., 2014a. Two novel simian arteriviruses in captive and wild baboons (Papio spp.). J. Virol. 88 (22), 13231–13239.

Bailey, A.L., Lauck, M., Weiler, A., Sibley, S.D., Dinis, J.M., Bergman, Z., Nelson, C.W., Correll, M., Gleicher, M., Hyeroba, D., Tumukunde, A., Weny, G., Chapman, C., Kuhn, J.H., Hughes, A.L., Friedrich, T.C., Goldberg, T.L., O'Connor, D.H., 2014b. High genetic diversity and adaptive potential of two simian hemorrhagic fever viruses in a wild primate population. PLOS ONE 9 (3), e90714.

Beerens, N., Selisko, B., Ricagno, S., Imbert, I., van der Zanden, L., Snijder, E.J., Canard, B., 2007. De novo initiation of RNA synthesis by arterivirus RNA-dependent RNA polymerase. J. Virol. 81 (16), 8384–8395.

Beura, L.K., Sarkar, S.N., Kwon, B., Subramaniam, S., Jones, C., Pattnaik, A.K., Osorio, F.A., 2010. Porcine reproductive and respiratory syndrome virus nonstructural protein 1beta modulates host innate immune response by antagonizing IRF3 activation. J. Virol. 84 (3), 1574–1584.

Beura, L.K., Subramaniam, S., Vu, H.L., Kwon, B., Pattnaik, A.K., Osorio, F.A., 2012. Identification of amino acid residues important for anti-IFN activity of porcine reproductive and respiratory syndrome virus non-structural protein 1. Virology 433 (2), 431–439.

Bray, M., Geisbert, T.W., 2005. Ebola virus: the role of macrophages and dendritic cells in the pathogenesis of Ebola hemorrhagic fever. Int. J. Biochem. Cell Biol. 37 (8), 1560–1566.

Cai, Y., Postnikova, E.N., Bernbaum, J.G., Yu, S.Q., Mazur, S., Deiuliis, N.M., Radoshitzky, S.R., Lackemeyer, M.G., McCluskey, A., Robinson, P.J., Haucke, V., Wahl-Jensen, V., Bailey, A.L., Lauck, M., Friedrich, T.C., O'Connor, D.H., Goldberg, T.L., Jahrling, P.B., Kuhn, J.H., 2014. Simian hemorrhagic fever virus cell entry is dependent on CD163 and uses a clathrin-mediated endocytosis-like pathway. J. Virol. (Oct 29), pii: JVI.02697-14. [Epub ahead of print].

Delputte, P.L., Van Breedam, W., Delrue, I., Oetke, C., Crocker, P.R., Nauwynck, H.J., 2007. Porcine arterivirus attachment to the macrophage-specific receptor sialoadhesin is dependent on the sialic acid-binding activity of the N-terminal immunoglobulin domain of sialoadhesin. J. Virol. 81 (17), 9546–9550.

Delputte, P.L., Vanderheijden, N., Nauwynck, H.J., Pensaert, M.B., 2002. Involvement of the matrix protein in attachment of porcine reproductive and respiratory syndrome virus to a heparin like receptor on porcine alveolar macrophages. J. Virol. 76 (9), 4312–4320.

den Boon, J.A., Faaberg, K.S., Meulenberg, J.J., Wassenaar, A.L., Plagemann, P.G., Gorbalenya, A.E., Snijder, E.J., 1995. Processing and evolution of the N-terminal region of the arterivirus replicase ORF1a protein: identification of two papain like cysteine proteases. J. Virol. 69 (7), 4500–4505.

Dunowska, M., Biggs, P.J., Zheng, T., Perrott, M.R., 2012. Identification of a novel nidovirus associated with a neurological disease of the Australian brushtail possum (*Trichosurus vulpecula*). Vet. Microbiol. 156 (3–4), 418–424.

Fang, Y., Snijder, E.J., 2010. The PRRSV replicase: exploring the multifunctionality of an intriguing set of nonstructural proteins. Virus Res. 154 (1–2), 61–76.

Fang, Y., Treffers, E.E., Li, Y., Tas, A., Sun, Z., van der Meer, Y., de Ru, A.H., van Veelen, P.A., Atkins, J.F., Snijder, E.J., Firth, A.E., 2012. Efficient −2 frameshifting by mammalian ribosomes to synthesize an additional arterivirus protein. Proc. Natl. Acad. Sci. U. S. A. 109 (43), E2920–E2928.

Godeny, E.K., deVries, A.A.F., Wang, X.C., Smith, S.L., deGroot, R.J., 1998. Identification of the leader-body junctions for the viral subgenomic mRNAs and organization of the simian hemorrhagic fever virus genome: evidence for gene duplication during arterivirus evolution. J. Virol. 72 (1), 862–867.

Gravell, M., London, W.T., Leon, M.E., Palmer, A.E., Hamilton, R.S., 1986. Differences among isolates of simian hemorrhagic fever (SHF) virus. Proc. Soc. Exp. Biol. Med. 181 (1), 112–119.

Han, M., Kim, C.Y., Rowland, R.R., Fang, Y., Kim, D., Yoo, D., 2014. Biogenesis of nonstructural protein 1 (nsp1) and nsp1-mediated type I interferon modulation in arteriviruses. Virology 458–459, 136–150.

Johnson, C.R., Griggs, T.F., Gnanandarajah, J., Murtaugh, M.P., 2011a. Novel structural protein in porcine reproductive and respiratory syndrome virus encoded by an alternative ORF5 present in all arteriviruses. J. Gen. Virol. 92 (Pt 5), 1107–1116.

Johnson, R.F., Dodd, L.E., Yellayi, S., Gu, W., Cann, J.A., Jett, C., Bernbaum, J.G., Ragland, D.R., St Claire, M., Byrum, R., Paragas, J., Blaney, J.E., Jahrling, P.B., 2011b. Simian hemorrhagic fever virus infection of rhesus macaques as a model of viral hemorrhagic fever: clinical characterization and risk factors for severe disease. Virology 421 (2), 129–140.

Kim, O., Sun, Y., Lai, F.W., Song, C., Yoo, D., 2010. Modulation of type I interferon induction by porcine reproductive and respiratory syndrome virus and degradation of CREB-binding protein by non-structural protein 1 in MARC-145 and HeLa cells. Virology 402 (2), 315–326.

Kroese, M.V., Zevenhoven-Dobbe, J.C., Bos-de Ruijter, J.N., Peeters, B.P., Meulenberg, J.J., Cornelissen, L.A., Snijder, E.J., 2008. The nsp1alpha and nsp1 papain-like autoproteinases are essential for porcine reproductive and respiratory syndrome virus RNA synthesis. J. Gen. Virol. 89 (Pt 2), 494–499.

Lapin, B.A., Shevtsova, Z.V., 1971. On the identity of two simian hemorrhagic fever virus strains (Sukhumi and NIH). Z. Versuchstierkd. 13 (1), 21–23.

Lauck, M., Hyeroba, D., Tumukunde, A., Weny, G., Lank, S.M., Chapman, C.A., O'Connor, D.H., Friedrich, T.C., Goldberg, T.L., 2011. Novel, divergent simian hemorrhagic fever viruses in a wild Ugandan red colobus monkey discovered using direct pyrosequencing. PLoS ONE 6 (4), e19056.

Lauck, M., Sibley, S.D., Hyeroba, D., Tumukunde, A., Weny, G., Chapman, C.A., Ting, N., Switzer, W.M., Kuhn, J.H., Friedrich, T.C., O'Connor, D.H., Goldberg, T.L., 2013. Exceptional simian hemorrhagic fever virus diversity in a wild African primate community. J. Virol. 87 (1), 688–691.

Lee, C., Yoo, D., 2006. The small envelope protein of porcine reproductive and respiratory syndrome virus possesses ion channel protein-like properties. Virology 355, 30–43.

London, W.T., 1977. Epizootiology, transmission and approach to prevention of fatal simian haemorrhagic fever in rhesus monkeys. Nature 268 (5618), 344–345.

Mahanty, S., Bray, M., 2004. Pathogenesis of filoviral haemorrhagic fevers. Lancet Infect. Dis. 4 (8), 487–498.

Maines, T.R., Young, M., Dinh, N.N., Brinton, M.A., 2005. Two cellular proteins that interact with a stem loop in the simian hemorrhagic fever virus 3′(+)NCR RNA. Virus Res. 109 (2), 109–124.
Mielech, A.M., Chen, Y., Mesecar, A.D., Baker, S.C., 2014. Nidovirus papain-like proteases: multifunctional enzymes with protease, deubiquitinating and deISGylating activities. Virus Res. (Feb 7), http://dx.doi.org/10.1016/j.virusres.2014.01.025, pii: S0168-1702(14)00040-9. [Epub ahead of print].
Moore, K.W., de Waal Malefyt, R., Coffman, R.L., O'Garra, A., 2001. Interleukin-10 and the interleukin-10 receptor. Annu. Rev. Immunol. 19, 683–765.
Nedialkova, D.D., Gorbalenya, A.E., Snijder, E.J., 2010. Arterivirus Nsp1 modulates the accumulation of minus-strand templates to control the relative abundance of viral mRNAs. PLoS Pathog. 6 (2), e1000772.
Palmer, A.E., Allen, A.M., Tauraso, N.M., Shelokov, A., 1968. Simian hemorrhagic fever. I. Clinical and epizootiologic aspects of an outbreak among quarantined monkeys. Am. J. Trop. Med. Hyg. 17 (3), 404–412.
Renquist, D., 1990. Outbreak of simian hemorrhagic fever. J. Med. Primatol. 19 (1), 77–79.
Shevtsova, Z.V., 1969. A further study of simian hemorrhagic fever virus. Vopr. Virusol. 14 (5), 604–607.
Snijder, E.J., Kikkert, M., 2013. In: Knipe, D.M., Howley, P.M. (Eds.), Arteriviruses. Fields Virology, vol. 1. Lippincott, Williams and Wilkins, Philadelphia, PA, pp. 859–879.
Snijder, E.J., Meulenberg, J.J.M., 1998. The molecular biology of arterivirus. J. Gen. Virol. 79, 961–979.
Snijder, F E.J., Spaan, W.J.M., 2006. In: Knipe, D.M., Howley, P.M. (Eds.), Arterivirus. Fields Virology, vol. 1, 5th ed. Lippincott, Williams and Wilkins, Philadelphia, PA, pp. 1337–1355.
Snijder, E.J., van Tol, H., Pedersen, K.W., Raamsman, M.J., de Vries, A.A., 1999. Identification of a novel structural protein of arteriviruses. J. Virol. 73 (8), 6335–6345.
Snijder, E.J., Wassenaar, A.L., Spaan, W.J., 1992. The 5′ end of the equine arteritis virus replicase gene encodes a papain like cysteine protease. J. Virol. 66 (12), 7040–7048.
Song, C., Krell, P., Yoo, D., 2010. Nonstructural protein 1alpha subunit-based inhibition of NF-kappaB activation and suppression of interferon-beta production by porcine reproductive and respiratory syndrome virus. Virology 407 (2), 268–280.
Sun, L., Li, Y., Liu, R., Wang, X., Gao, F., Lin, T., Huang, T., Yao, H., Tong, G., Fan, H., Wei, Z., Yuan, S., 2013. Porcine reproductive and respiratory syndrome virus ORF5a protein is essential for virus viability. Virus Res. 171 (1), 178–185.
Sun, Y., Xue, F., Guo, Y., Ma, M., Hao, N., Zhang, X.C., Lou, Z., Li, X., Rao, Z., 2009. Crystal structure of porcine reproductive and respiratory syndrome virus leader protease Nsp1alpha. J. Virol. 83 (21), 10931–10940.
Tauraso, N.M., Shelokov, A., Palmer, A.E., Allen, A.M., 1968. Simian hemorrhagic fever. 3. Isolation and characterization of a viral agent. Am. J. Trop. Med. Hyg. 17 (3), 422–431.
Thaa, B., Kabatek, A., Zevenhoven-Dobbe, J.C., Snijder, E.J., Herrmann, A., Veit, M., 2009. Myristoylation of the arterivirus E protein: the fatty acid modification is not essential for membrane association but contributes significantly to virus infectivity. J. Gen. Virol. 90 (Pt 11), 2704–2712.
Tian, D., Wei, Z., Zevenhoven-Dobbe, J.C., Liu, R., Tong, G., Snijder, E.J., Yuan, S., 2012. Arterivirus minor envelope proteins are a major determinant of viral tropism in cell culture. J. Virol. 86 (7), 3701–3712.
van Berlo, M.F., Horzinek, M.C., van der Zeijst, B.A., 1982. Equine arteritis virus-infected cells contain six polyadenylated virus-specific RNAs. Virology 118 (2), 345–352.
Van Breedam, W., Delputte, P.L., Van Gorp, H., Misinzo, G., Vanderheijden, N., Duan, X., Nauwynck, H.J., 2010. Porcine reproductive and respiratory syndrome virus entry into the porcine macrophage. J. Gen. Virol. 91 (Pt 7), 1659–1667.
van Dinten, L.C., den Boon, J.A., Wassenaar, A.L., Spaan, W.J., Snijder, E.J., 1997. An infectious arterivirus cDNA clone: identification of a replicase point mutation that abolishes discontinuous mRNA transcription. Proc. Natl. Acad. Sci. U. S. A. 94 (3), 991–996.
van Kasteren, P.B., Bailey-Elkin, B.A., James, T.W., Ninaber, D.K., Beugeling, C., Khajehpour, M., Snijder, E.J., Mark, B.L., Kikkert, M., 2013. Deubiquitinase function of arterivirus papain-like protease 2 suppresses the innate immune response in infected host cells. Proc. Natl. Acad. Sci. U. S. A. 110 (9), E838–E847.
Vatter, H.A., Brinton, M.A., 2014. Differential responses of disease-resistant and disease-susceptible primate macrophages and myeloid dendritic cells to simian hemorrhagic fever virus infection. J. Virol. 88 (4), 2095–2106.
Vatter, H.A., Di, H., Donaldson, E.F., Baric, R.S., Brinton, M.A., 2014a. Each of the eight simian hemorrhagic fever virus minor structural proteins is functionally important. Virology 462–463, 351–362.
Vatter, H.A., Di, H., Donaldson, E.F., Radu, G.U., Maines, T.R., Brinton, M.A., 2014b. Functional analyses of the three simian hemorrhagic fever virus nonstructural protein 1 papain-like proteases. J. Virol. 88 (16), 9129–9140.
Vatter, H.A., Donaldson, E.F., Huynh, J., Rawlings, S., Manoharan, M., Legasse, A., Planar, S., Dickerson, M.F., Lewis, A.D., Colgin, L., Axthelm, M.K., Poteet, J.K., Baric, R.S., Wong, S.W., Brinton, M.A., 2015. A simian hemorrhagic fever virus isolate from persistently infected baboons efficiently induces hemorrhagic fever disease in Japanese macaques. Virology 474, 186–196.
Welch, S.K., Calvert, J.G., 2010. A brief review of CD163 and its role in PRRSV infection. Virus Res. 154 (1–2), 98–103.
Xue, F., Sun, Y., Yan, L., Zhao, C., Chen, J., Bartlam, M., Li, X., Lou, Z., Rao, Z., 2010. The crystal structure of porcine reproductive and respiratory syndrome virus nonstructural protein Nsp1beta reveals a novel metal-dependent nuclease. J. Virol. 84 (13), 6461–6471.
You-Kyung, Brinton, M.A., 1998. A 68-nucleotide sequence within the 3′ noncoding region of simian hemorrhagic fever virus negative-strand RNA binds to four MA104 cell proteins. J. Virol. 72 (5), 4341–4351.
Zeng, L., Godeny, E.K., Methven, S.L., Brinton, M.A., 1995. Analysis of simian hemorrhagic fever virus (SHFV) subgenomic RNAs, junction sequences, and 5′ leader. Virology 207 (2), 543–548.
Ziebuhr, J., Snijder, E.J., Gorbalenya, A.E., 2000. Virus-encoded proteinases and proteolytic processing in the Nidovirales. J. Gen. Virol. 81 (Pt 4), 853–879.